Available online at www.sciencedirect.com
SCIENCE DIRECT
Nuclear Instruments and Methods in Physics Research B 249 (2006) 390–393
NIM B
Beam Interactions with Materials & Atoms
www.elsevier.com/locate/nimb

Observation of Si emission during thermal oxidation of Si(001) with high-resolution RBS

S. Hosoi [a,*], K. Nakajima [a], M. Suzuki [a], K. Kimura [a], Y. Shimizu [b], S. Fukatsu [b], K.M. Itoh [b], M. Uematsu [c], H. Kageshima [c], K. Shiraishi [d]

[a] Department of Micro Engineering, Kyoto University, Kyoto 606-8501, Japan
[b] Department of Applied Physics and Physico-Informatics and CREST-JST, Keio University, Yokohama 223-8522, Japan
[c] NTT Basic Research Laboratories, NTT Corporation, Atsugi 243-0198, Japan
[d] Institute of Physics, University of Tsukuba, Tsukuba 305-8571, Japan

Available online 13 June 2006

Abstract

An epitaxially grown Si isotope heterostructure, ^{28}Si(2 nm)/^{30}Si(1 nm)/^{nat}Si, was used to study the behavior of Si atoms during oxidation. The change in the Si-isotope profiles during the oxidation was observed using high-resolution Rutherford backscattering spectroscopy. A significant oxidation-enhanced diffusion of ^{30}Si into the ^{nat}Si layer was observed in the oxidation at 800 °C, while the concentration of emitted ^{30}Si into the $^{28}SiO_2$ layer was found to be less than 5 at.% in the oxidation at 1100 °C.

PACS: 61.18.Bn; 66.30.Xj

Keywords: Si emission; HRBS; Thermal oxidation; Si isotope; Diffusion; SiO_2

1. Introduction

With the downscaling of metal-oxide-semiconductor field effect transistors (MOS-FETs), the thickness of the gate oxide film is approaching to 1 nm. For precise control of the oxide thickness, understanding of the silicon oxidation mechanism is of prime importance. During oxidation, a significant volume expansion takes place because the volume occupied per Si atom in SiO_2 is about twice larger than that in Si. This volume expansion induces extremely high stress at the SiO_2/Si interface. The induced stress should be released for further oxidation. This can be done by Si emission from the interface into either the Si substrate or the SiO_2 layer. The oxidation-enhanced diffusion (OED) [1,2] and the oxidation-induced stacking faults [3–5], are known to be related to the Si emission into the Si substrate.

Recent theoretical studies have shown that Si species are emitted not only into the Si substrate but also into the SiO_2 layer [6–8]. Taking into account the Si emission, the oxidation rate was explained in the full thickness range [7]. There were several experimental studies suggesting the Si emission into the SiO_2 layer [9–12], although no direct observation has been reported so far. In the present paper, we observe the behavior of Si atoms during oxidation using Si isotopes. The motion of ^{30}Si is traced using high-resolution Rutherford backscattering spectroscopy (HRBS).

2. Experimental

A Si isotope heterostructure (^{28}Si/^{30}Si/^{nat}Si) was prepared by the following procedure at Keio university [13,14]. After the native oxide was removed by a dilute HF solution, a buffer layer of ^{nat}Si (100 nm) was epitaxially grown on a 2-in wafer of natural Si(001) by electron beam evaporation. Subsequently, ^{30}Si and ^{28}Si layers were grown at 650 °C by molecular beam epitaxy. The nominal

* Corresponding author. Tel.: +81 75 753 5268; fax: +81 75 753 5253.
E-mail address: shigetaka-h@t01.mbox.media.kyoto-u.ac.jp (S. Hosoi).

0168-583X/$ - see front matter © 2006 Elsevier B.V. All rights reserved.
doi:10.1016/j.nimb.2006.04.036

thicknesses of the ^{30}Si and ^{28}Si layers were 1 and 2 nm, respectively. The prepared heterostructure wafer was divided into several pieces of 1×1 cm^2. These pieces were oxidized in an infrared furnace in an oxygen atmosphere (pressure of 100 kPa), and depth profiles of isotopes were measured using HRBS.

The details of the HRBS measurement were described elsewhere [15]. Briefly, a beam of 400 keV He^+ ions was collimated to 2×2 mm^2 and to a divergence angle of less than 0.1° by a series of slit systems. The ion beam was incident on the sample at an incident angle of 15°, and the He^+ ions scattered at 100° were energy analyzed by a 90° sector magnetic spectrometer. The depth resolution is estimated to be ~0.4 nm at surface and ~0.8 nm at a depth of 2 nm.

It should be noted that ^{30}Si atoms may diffuse into the crystalline ^{28}Si layer due to OED during the initial oxidation of the ^{28}Si layer. These ^{30}Si atoms cannot be distinguished from the ^{30}Si atoms emitted into $^{28}SiO_2$ layer during the oxidation of the ^{30}Si layer. In order to avoid this problem, the ^{28}Si layer was oxidized at a relatively low temperature (800 °C) to prevent OED. After oxidation of the ^{28}Si layer, ^{30}Si layer was oxidized at a higher temperature (1100 °C). The HRBS measurements were performed before and after the second oxidation. Comparing these HRBS spectra, the behavior of ^{30}Si atoms during the oxidation of ^{30}Si layer can be seen.

3. Results and discussion

Fig. 1 shows the observed HRBS spectrum of an as-grown sample. There are three sharp peaks at ~219, ~284 and ~289 keV. The peak at ~289 keV is the signal from the ^{30}Si layer, and the peak at ~284 keV corresponds to the ^{28}Si layer. A small peak seen at ~219 keV corresponds to the oxygen in a thin native $^{28}SiO_2$. The signal from the ^{nat}Si layer appears below ~283 keV. Elemental depth profiles were determined through simulations of HRBS spectrum. The simulated HRBS spectrum is shown by a solid curve. The contributions of ^{nat}Si, ^{28}Si, ^{30}Si and O are also shown by dotted, dashed, long-dashed and dot-dashed curves, respectively.

The derived depth profiles are shown in the inset of Fig. 1. By integrating these profiles, the amounts of ^{28}Si and ^{30}Si are estimated to be 9.7×10^{15} and 5.0×10^{15} atoms/cm^2, respectively, which correspond to thicknesses of 1.9 and 1.0 nm. These profiles indicate that the Si isotope heterostructure was grown as was designed. The Si isotope layers are rather uniform although a weak intermixing between the adjacent epitaxial layers occurs.

The energy spectrum of the sample after oxidization at 800 °C for 3 min is shown in Fig. 2. After oxidation, the oxygen and ^{28}Si peaks become broader, while the ^{30}Si peak stays almost unchanged. This suggests that only the ^{28}Si layer was oxidized as was intended. The derived depth profiles of the elements and isotopes (the inset of Fig. 2) confirm this. Comparing the depth profiles with those observed before oxidation (the inset of Fig. 1), the behavior of Si isotopes during the oxidation of ^{28}Si layer can be seen. The direct comparison of these profiles, however, is meaningless because the thickness of the isotope layers was changed by oxidation.

If there is no emission and no diffusion during the oxidation, the depth profiles of elements and isotopes after oxidation can be calculated from the depth profiles measured before oxidation. In the calculation, we assumed that the oxygen profile is the same as that observed after oxidation and the concentration ratio between ^{28}Si and ^{30}Si does not change due to the oxidation. Comparing these profiles with those measured after oxidation, the behavior of the Si isotopes can be clearly seen. Fig. 3 shows the comparison between the calculated ^{30}Si profile (dashed curve) and that measured after oxidation (solid curve). It can be seen that ^{30}Si atoms diffuse into the ^{nat}Si layer during the oxidation of the ^{28}Si layer with a diffusion length of about

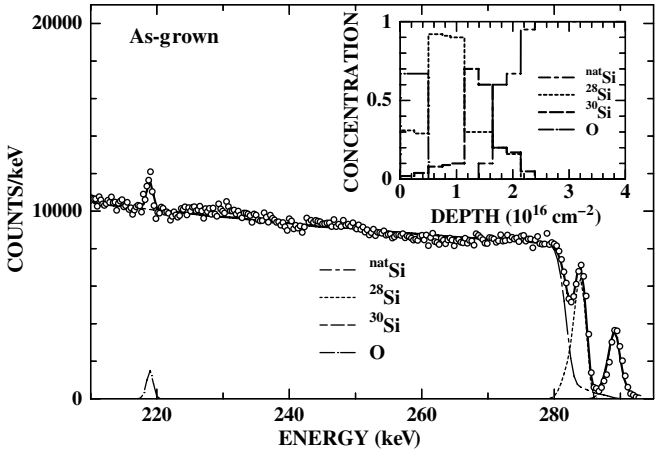

Fig. 1. Observed HRBS spectrum for the as-grown sample. Elemental depth profiles determined through simulations of the HRBS spectrum are shown in the inset. A native SiO_2 layer of 0.7 nm thickness and weak intermixing between the adjacent epitaxial layers can be observed.

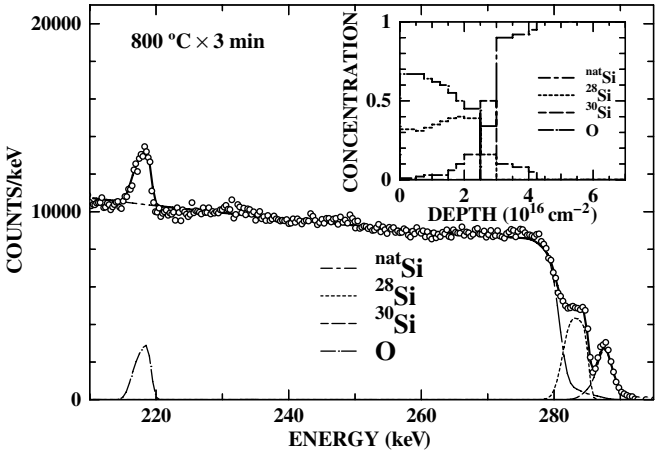

Fig. 2. Observed HRBS spectrum after the first oxidation (800 °C × 3 min). Elemental depth profiles determined through simulations of the HRBS spectrum are shown in the inset. The ^{28}Si layer is almost completely oxidized while the ^{30}Si layer is only slightly oxidized.

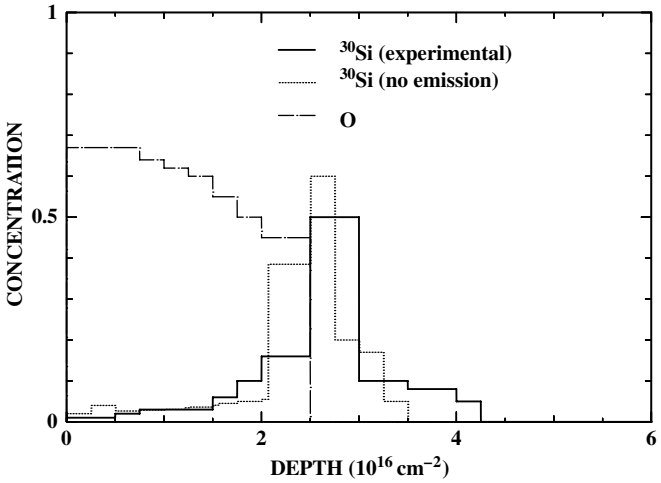

Fig. 3. Depth profile of ^{30}Si after the first oxidation calculated from the profile measured before oxidation (see text). Depth profiles of ^{30}Si and O measured after the first oxidation are also shown for comparison. It can be seen that ^{30}Si atoms diffuse into the ^{nat}Si layer during the oxidation.

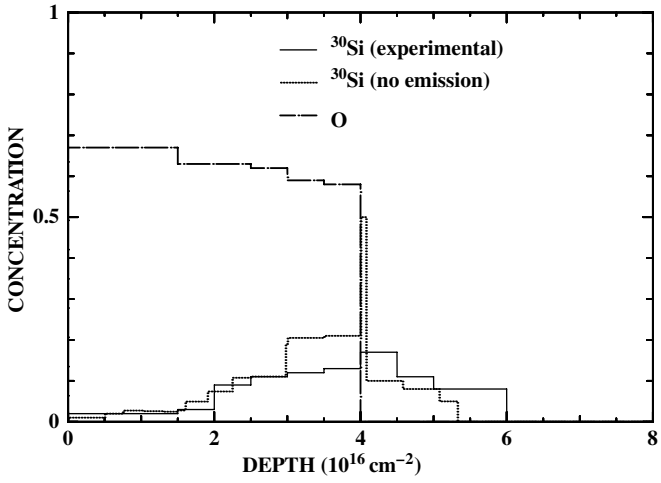

Fig. 5. Depth profile of ^{30}Si after the second oxidation calculated from the profile measured before the second oxidation (see text). Depth profiles of ^{30}Si and O measured after the second oxidation are also shown for comparison. It can be seen that ^{30}Si atoms diffuse into the ^{nat}Si layer during the oxidation, while no ^{30}Si emission into the $^{28}SiO_2$ layer is observed within the experimental error.

1.5 nm (8×10^{15} atoms/cm^2). The diffusion coefficient estimated from the observed diffusion length is $\sim3\times10^{-17}$ cm^2/s. This is about 1000 times larger than the Si self-diffusion coefficient reported in literatures [16]. This surprisingly large enhancement is ascribed to OED. Assuming that the enhancement is proportional to the interstitial concentration [17] and using the equilibrium interstitial concentration ($\sim3\times10^{9}$ cm^{-3}) given in the literature [18], the Si interstitial concentration in the ^{30}Si and ^{nat}Si layers during the oxidation of the ^{28}Si layer is estimated to be $\sim3\times10^{12}$ cm^{-3}.

Fig. 4 shows the HRBS spectrum observed after additional oxidation at 1100 °C for 5 s. The oxygen peak becomes much broader and the broadening of the ^{30}Si peak is also clearly seen, indicating that the ^{30}Si layer was oxidized. The depth profiles derived from the spectrum are shown in the inset. In order to see the motion of ^{30}Si atoms during the oxidation, the ^{30}Si profile was calculated from that observed after the first oxidation (800 °C × 3 min) assuming that there is no diffusion and no emission. The comparison between the calculated profile and the observed one is shown in Fig. 5. The diffusion of ^{30}Si atoms into the ^{nat}Si layer is seen again in this case. A rough estimate gives the diffusion coefficient of $\sim1\times10^{-15}$ cm^2/s, which is roughly in agreement with the equilibrium diffusion coefficient reported in the literatures [16].

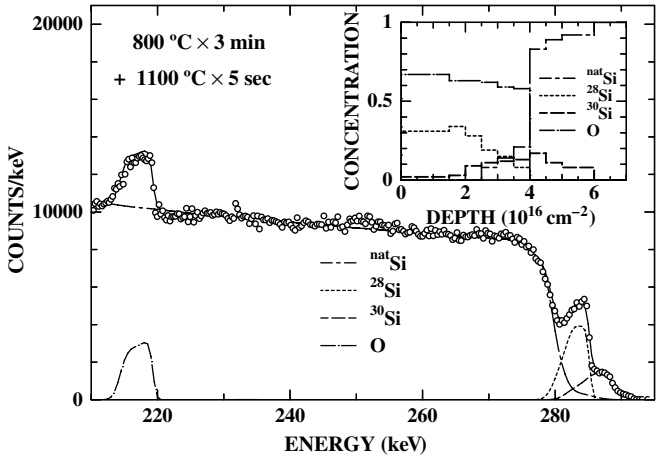

Fig. 4. Observed HRBS spectrum after the second oxidation (1100 °C × 5 s). Elemental depth profiles determined through simulations of the HRBS spectrum are shown in the inset. Both ^{28}Si and ^{30}Si layers are almost completely oxidized.

Regarding the ^{30}Si emission, the ^{30}Si profile in the $^{28}SiO_2$ layer ($0–3\times10^{16}$ atoms/cm^2) does not change within the experimental uncertainty (±5 at.%). Thus, it is concluded that the ^{30}Si emission into the $^{28}SiO_2$ layer is less than 5 at.% in the present conditions. This is not in contradiction to the theoretical prediction because the predicted amount of emitted ^{30}Si is about 2 at.% in the $^{28}SiO_2$ layer in the present case [19]. More detailed measurements are required for the observation of the predicted Si emission.

4. Conclusion

An epitaxially grown Si isotope heterostructure, ^{28}Si-(2 nm)/^{30}Si(1 nm)/^{nat}Si, has been used to measure the behavior of Si atoms during oxidation. The heterostructure was oxidized in O_2 (100 kPa) and the isotope profiles were observed using HRBS. Significant oxidation-enhanced diffusion was observed in oxidation at 800 °C, while the ^{30}Si emission into the SiO_2 layer was not observed within the experimental error (±5 at.%).

Acknowledgement

This work was supported in part by "Nanotechnology Support Project" and the Special Coordination Funds for

Promoting Science and Technology from the Ministry of Education, Culture, Sports, Science and Technology. This work was also supported by the Center of Excellence for Research and Education on Complex Functional Mechanical Systems (COE program) of the Ministry of Education, Culture, Sports, Science and Technology.

References

[1] S. Mizuo, H. Higuchi, Jpn. J. Appl. Phys. 20 (1981) 739.
[2] T.Y. Tan, U. Gosele, Appl. Phys. A 37 (1985) 1.
[3] D.J.D. Thomas, Phys. Status Solidi 3 (1963) 2261.
[4] K.V. Ravi, C.J. Varker, J. Appl. Phys. 45 (1974) 263.
[5] S.M. Hu, Appl. Phys. Lett. 27 (1975) 165.
[6] H. Kageshima, K. Shiraishi, Phys. Rev. Lett. 81 (1998) 5936.
[7] H. Kageshima, K. Shiraishi, M. Uematsu, Jpn. J. Appl. Phys. 38 (1999) L971.
[8] M. Uematsu, H. Kageshima, Y. Takahashi, S. Fukatsu, K.M. Itoh, K. Shiraishi, U. Gosele, Appl. Phys. Lett. 84 (2004) 876.
[9] G.K. Celler, L.E. Trimble, Appl. Phys. Lett. 54 (1989) 1427.
[10] Y. Takakuwa, M. Nihei, N. Miyamoto, Appl. Surf. Sci. 117–118 (1997) 141.
[11] S. Fukatsu, T. Takahashi, K.M. Itoh, M. Uematsu, A. Fujiwara, H. Kageshima, Y. Takahashi, K. Shiraishi, U. Gosele, Appl. Phys. Lett. 83 (2003) 3897.
[12] S. Fukatsu, K.M. Itoh, M. Uematsu, H. Kageshima, Y. Takahashi, K. Shiraishi, Jpn. J. Appl. Phys. 43 (2004) 7837.
[13] K.M. Itoh, J. Kato, M. Uemura, A.K. Kaliteevskii, O.N. Godisov, G.G. Devyatych, A.D. Bulanov, A.V. Gusev, I.D. Kovalev, P.G. Sennikov, H.-J. Pohl, N.V. Abrosimov, H. Riemann, Jpn. J. Appl. Phys. 42 (2003) 6248.
[14] T. Kojima, R. Nebashi, K.M. Itoh, Y. Shiraki, Appl. Phys. Lett. 83 (2003) 2318.
[15] K. Kimura, K. Ohshima, M. Mannami, Appl. Phys. Lett. 64 (1994) 2232.
[16] A. Ural, P.B. Griffin, J.D. Plummer, Phys. Rev. Lett. 83 (1999) 3454, and reference therein.
[17] P.M. Fahey, P.B. Griffin, J.D. Plummer, Rev. Mod. Phys. 61 (1989) 289.
[18] H. Bracht, N.A. Stolwijk, H. Mehrer, Phys. Rev. B 52 (1995) 16542.
[19] M. Uematsu, H. Kageshima, K. Shiraishi, Jpn. J. Appl. Phys. 39 (2000) L699.